Journal of Statistical Physics, Vol. 108, Nos. 5/6, September 2002 (© 2002)

Particle Dynamics in Time-Dependent Stadium-Like Billiards

Alexander Loskutov[1] **and Alexei Ryabov**[1]

Received November 7, 2001; accepted April 25, 2002

Billiards in the form of a stadium with perturbed boundaries are considered. Investigations are primarily devoted to billiards having a near-rectangle form, but the results regarding the "classical" stadium with the boundary that consists of two semicircles and two parallel segments tangent to them, are also described. In the phase plane, areas corresponding to decrease and increase of the velocity of billiard particles are found. The average velocity of the particle ensemble as a function of the number of collisions with the boundary is obtained.

KEY WORDS: Billiards; chaos; phase portraits; Fermi acceleration.

1. INTRODUCTION

The notion of billiard dynamical systems is known in physics since Bikhoff[(1)] who considered a problem concerning the free motion of a point particle (billiard ball) in some bounded manifold. The billiard dynamical system can be introduced as follows. A billiard table Q is a Riemannian manifold M with a piecewise smooth boundary ∂Q. The billiard particle moves freely in Q. Upon reaching the boundary, it is reflected from it elastically. Thus, the billiard particle moves along geodesic lines with a constant velocity. In the present article we consider billiards in Euclidean plane.

In accordance with the boundary geometry, dynamics of the billiard particle can be integrable,[(2)] completely chaotic[(3, 4)] or, depending on the initial conditions, regular or chaotic.[(5–8)]

If the set ∂Q is not perturbed with time then such billiard systems are said to be billiards with a fixed (constant) boundary. In the case of $\partial Q = \partial Q(t)$ the corresponding billiards are called billiards with time-dependent

[1] Physics Faculty, Moscow State University, Moscow 119899, Russia; e-mail: loskutov@moldyn.phys.msu.su

0022-4715/02/0900-0995/0 © 2002 Plenum Publishing Corporation

boundaries. For the most part, investigations of classical time-dependent billiards concerned two main questions: descriptions of their statistical properties and the study of trajectories for which the particle velocity grows indefinitely. This problem is related to the unbounded increase of energy in periodically forced Hamiltonian systems and known as Fermi acceleration.[9, 10]

The Fermi–Ulam model was the first system where invariant curves, chaotic layers and stable islands have been investigated (details see in ref. 11). It has been shown that in the case of a quite smooth boundary perturbation the growth of the particle velocity is bounded. Otherwise, the velocity can increase indefinitely.

For two-dimensional time-dependent billiards, the problem of Fermi acceleration have been investigated in refs. 12 and 13. *Integrable* billiard systems in circles and ellipses have been studied in refs. 2, 12, 14, and 15). In these papers, the authors came to conclusion that the velocity of the particle ensemble is always bounded. Investigations of *chaotic* billiards have been performed for the Lorentz gas.[16, 17] As predicted, perturbations of the boundary in such billiards lead to the appearance the Fermi acceleration. Moreover, the acceleration is higher for the in-phase periodical oscillations of the scatterers than for their stochastic perturbations. The necessary conditions for the existence of chaos in vibrating quantum billiards on Riemannian manifolds are described in ref. 18. Quantum chaos in rectangular and spherical vibrating billiards have been investigated in ref. 19 and 20).

In the present paper, we study so-called stadium-like billiards[8] which are defined as a closed domain Q with the boundary ∂Q consisting of two focusing curves connected by the two parallel lines (see Fig. 1). If

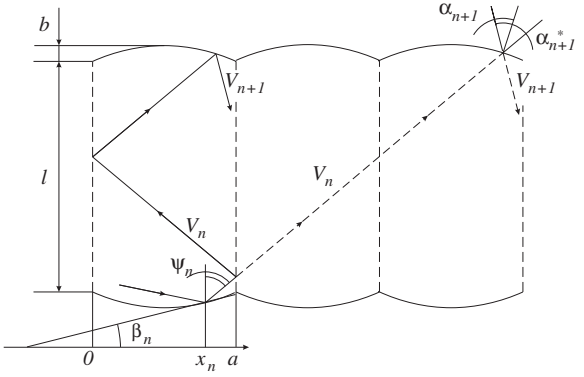

Fig. 1. A stadium-like billiard and its development.

parameter b is a sufficiently small then the billiard is a near-integrable system with stable fixed points. Therefore, in the stochastic "sea," the stability regions appear which consist of invariant curves. At the same time, owing to a weak nonlinearity, dynamics near separatrixes is stochastic, and the particles can reach neighbourhoods of all points in the stochastic layer. Thus, for the billiards with the fixed boundary, the particle dynamics can be either stochastic or regular. Introduction of external perturbations leads to the possibility of the passage of particles from the stochastic region to the regular one and back. As a result, new interesting phenomena appear which are also described in the paper.

2. DEFINITIONS AND MAPS

In this section, basic analytical results are presented. They are necessary for the further description of the billiard dynamics.

2.1. Stadium-Like Billiard with Fixed Parabolic Focusing Components

Consider a billiard shown in Fig. 1. To describe its dynamics let us construct the corresponding billiard map for $b \ll a$. To this end, one can use the well known method of specular reflections. As a result, the stadium is replaced by a "caterpillar." One can show that in both systems the change of the particle velocity value is the same. Moreover, there is a one-to-one correspondence between trajectories of the initial billiard and the obtained "caterpillar."

Suppose that the particle belongs to the billiard boundary and the velocity vector directs towards the interior of the billiard region Q. Let us choose coordinates ψ and x as shown in Fig. 1. The motion of the billiard particle generates a map $(\psi_n, x_n) \to (\psi_{n+1}, x_{n+1})$. Suppose that $b \ll l$. In this case the focusing components can be approximated by the function $\chi(x) = 4bx(x-a)/a^2$. For such a billiard system the map is written as follows:

$$x_{n+1} = x_n + l \tan \psi_{n+1} \pmod a,$$
$$\psi_{n+1} = \psi_n - 2\beta(x_{n+1}),$$

where $\beta(x) = \arctan(\chi'(x))$ (see Fig. 1). If b is small then $\beta \approx 4b(2x-a)/a^2$. For the further analysis let $\xi = x/a$, $\xi \in [0, 1)$. Then

$$\xi_{n+1} = \xi_n + \frac{l}{a} \tan \psi_n \pmod 1,$$
$$\psi_{n+1} = \psi_n - \frac{8b}{a}(2\xi_{n+1} - 1). \tag{1}$$

In Fig. 2 the phase portrait of the map (1) is shown. Initial conditions for each trajectory are marked by crosses. It is obvious that the fixed points of the map (1) corresponding to the family of large ellipses are the following: $\xi = 1/2$, $\tilde{\psi}^m = \arctan(ma/l)$. So, $m = 0$ corresponds to the first ellipse. In this case the particle moves strictly vertically (see Fig. 1). If $m = 1$ then the particle is shifted right by one segment. And so on. For example, in Fig. 1 the case of $m = 2$ is shown.

Let us find the stability conditions of the fixed points. To this end, change of variables, $\xi_n = \Delta\xi_n + 1/2$, $\psi_n = \Delta\psi_n + \arctan(ma/l)$, and linearize the map. Then we get:

$$\Delta\xi_{n+1} = \Delta\xi_n + \frac{l}{a\cos^2\tilde{\psi}^m}\Delta\psi_n + O(\Delta\psi_n^2),$$

$$\Delta\psi_{n+1} = \Delta\psi_n - \frac{16b}{a}\Delta\xi_{n+1},$$

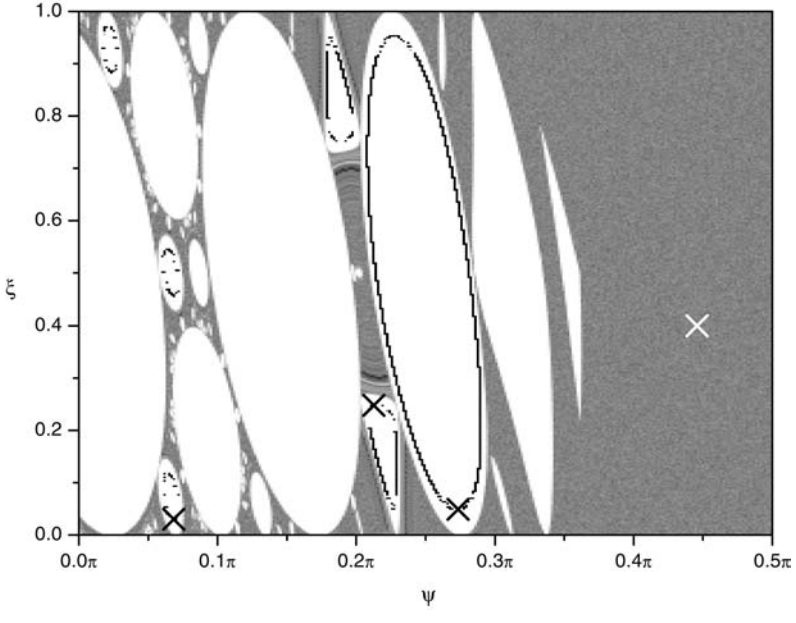

Fig. 2. Phase portrait of the billiard with parabolic focusing components (see map (1)) at $a = 0.5$, $b = 0.01$ and $l = 1$. The diagram contains three regular trajectories (each by 10^7 iterations) and one chaotic trajectory ($5 \cdot 10^8$ iterations).

where $\tilde{\psi}^m = \arctan(ma/l)$. The corresponding transformation matrix has the form:

$$A = \begin{pmatrix} 1 & \dfrac{l}{a\cos^2\tilde{\psi}^m} \\ -\dfrac{16b}{a} & 1-\dfrac{16bl}{a^2\cos^2\tilde{\psi}^m} \end{pmatrix}.$$

It is obvious that $\det A = 1$. Thus, the map preserves the phase volume.

The stability criterion for the fixed points is $|\mathrm{Tr}\, A| \leqslant 2$. Then $\cos^2\tilde{\psi}^m \geqslant 4bl/a^2$ or $m^2 \leqslant l/(4b) - l^2/a^2$. On the other hand, transition to chaos take place if

$$\frac{4bl}{a^2} > 1. \tag{2}$$

Eigenvalues of the matrix A are $\lambda_{1,2} = e^{\pm i\sigma}$, where $\cos\sigma = \frac{1}{2}\mathrm{Tr}\, A$. Let us introduce $f = l/(a\cos^2\tilde{\psi}^m)$, $g = 16b/a$. In this case

$$A = \begin{pmatrix} 1 & f \\ -g & 1-fg \end{pmatrix}$$

and its eigenvectors

$$X_{1,2} = \begin{pmatrix} 1 \\ \dfrac{e^{\pm i\sigma}-1}{f} \end{pmatrix}.$$

Consider the matrix X with the columns of eigenvectors. As known, in this case the matrix $\Lambda = X^{-1}AX$ is a diagonal one:

$$\Lambda = \begin{pmatrix} e^{i\sigma} & 0 \\ 0 & e^{-i\sigma} \end{pmatrix}.$$

New variables for which the transformation matrix has a diagonal form, are the following:

$$\begin{pmatrix} Z \\ Z^* \end{pmatrix} = X^{-1}\begin{pmatrix} \Delta\xi \\ \Delta\psi \end{pmatrix},$$

where

$$X^{-1} = \frac{i}{2\sin\sigma}\begin{pmatrix} e^{-i\sigma}-1 & -f \\ -e^{i\sigma}+1 & f \end{pmatrix}.$$

One can see that Z and Z^* are complex conjugated values. Thus,

$$Z_{n+1} = Z_n e^{i\sigma}.$$

If we take Z as $Z = Ie^{i\theta}$ then in the action–angle variables we obtain:

$$I_{n+1} = I_n,$$
$$\theta_{n+1} = \theta_n + \sigma,$$

where the rotation number is:

$$\sigma = \arccos\left(1 - \frac{8bl}{a^2\cos^2\tilde{\psi}^m}\right). \tag{3}$$

In turn, the inverse transformations have the form:

$$\Delta\xi = 2I\cos\theta,$$
$$\Delta\psi = \frac{2I}{f}(\cos(\sigma+\theta) - \cos\theta).$$

Therefore, the Jacobian of the transformation is the following: $J = -\frac{4I}{f}\sin\sigma$.

2.2. Perturbations of the Boundary and Resonance

Consider the particle trajectory near a fixed point. The time between two sequential collisions is the following: $\tau \approx \frac{l}{\cos\tilde{\psi}^m}\frac{1}{V}$. Thus, the rotation period is:

$$T_{\text{rot}} = \frac{2\pi}{\sigma}\tau = \frac{2\pi l}{\cos\tilde{\psi}^m \arccos\left(1 - 8bl/(a\cos\psi)^2\right)V}.$$

If the system undergoes external perturbations with period T_{ext}, then for $T_{\text{rot}} = T_{\text{ext}}$ we can observe a resonance. This leads to the possibility of the particle passages from the stochastic region to the regular one and back (see Fig. 2).

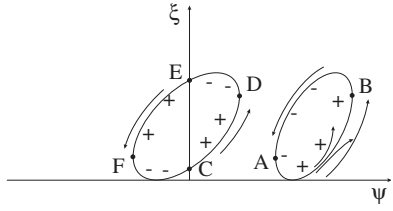

Fig. 3. Invariant curves around stable points (schematically).

The nature of the resonance (see Fig. 3) is the following. In the unperturbed billiards, at the motion along the invariant curve in the neighbourhood of a stable point, the angle ψ oscillates near the value of $\tilde{\psi}^m$. Collisions of the particle with the perturbed boundary leads to the change in ψ. If the boundary moves towards the particle, then the angle decreases. Otherwise it increases. Suppose that the trajectory moves along the arc AB. In this case, if the particle undergoes collisions coming from the opposite side, then the trajectory is shifted to the fixed point (to the ellipse center in Fig. 3). Otherwise, the particle trajectory tends to outside of the ellipse, i.e., to the stochastic layer.

From the equality $T_{\text{rot}} = T_{\text{ext}}$, we can obtain the resonance condition for the particle velocity:

$$V_r = \frac{l}{\cos\tilde{\psi}^m \arccos\left(1 - 8bl/(a\cos\tilde{\psi}^m)^2\right)}. \tag{4}$$

Hereafter, for simplicity we assume that the frequency of external perturbations $\omega = 1$. Then $T_{\text{ext}} = 2\pi$.

For the invariant curves with $\tilde{\psi}^m = \arctan(ma/l)$, $m \geqslant 1$, there exist two areas: an area where the absolute value of the angle ψ_n increases (along the arc AB from A to B in Fig. 3), and the area of the decrease in ψ_n. However, for the central stable fixed point there are two arcs: CD, EF for increasing and DE, FC for decreasing. Thus, for the resonance in a vicinity of this point, it is necessary that the particle velocity should be less by half. Therefore,

$$V_r^0 = \frac{V_r}{2} = \frac{l}{\arccos(1 - 8bl/a^2)}. \tag{5}$$

2.3. Focusing Components in the Form of the Circle Arcs

In previous sections, we used a quite rough map based on assumption $b \ll a, l$. In this section we construct an exact map for a stadium-like

billiard with the boundary consisting of two focusing components in the form of the circle arcs.

2.3.1. Fixed Boundary

Suppose that focusing components are circle arcs (symmetric about the vertical billiard axis) of the radius R with the angle measure 2Φ (Fig. 4). Geometrically one can obtain that

$$R = \frac{a^2 + 4b^2}{8b}; \qquad \Phi = \arcsin \frac{a}{2R}.$$

If the focusing component is a part of the circle C then in such a billiard the chaos can be observed when the disk D with $\partial D = C$ belongs to the billiard table Q.[21] Thus,

$$\frac{l}{2R} = \frac{4bl}{a^2} > 1,$$

that is the same as (2) obtained from the analysis of the stable points.

Let us introduce dynamical variables as shown in Fig. 4. Assume that angles φ_n and α_n^* are counted counterclockwise, and the angle α_n is counted clockwise. For the fixed boundary $\alpha_n^* = \alpha_n$. Suppose that V_n is the particle velocity, and t_n is a time of nth collision. Let us find a map describing dynamics of the particle in such a billiard system. Obviously, we should consider two cases: (1) After the collision with the focusing component the particle collides with the same boundary component (multiple collisions); (2) After the collision the particle moves to the opposite focusing component.

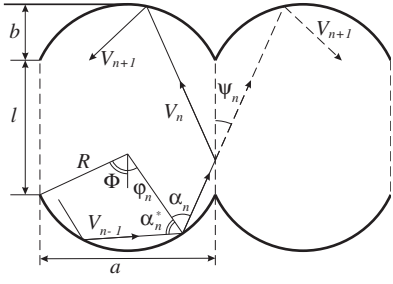

Fig. 4. A stadium-like billiard with focusing components in the form of the circle arcs.

(1) Multiple Collisions. In this case, geometrically we get the following map:

$$\begin{aligned}
\alpha^*_{n+1} &= \alpha_n, \\
\alpha_{n+1} &= \alpha^*_{n+1}, \\
\varphi_{n+1} &= \varphi_n + \pi - 2\alpha_n \pmod{2\pi}, \\
t_{n+1} &= t_n + \frac{2R\cos\alpha_n}{V_n}.
\end{aligned} \tag{6}$$

If $|\varphi_{n+1}| < \Phi$, then the particle collides with the same component. Otherwise, $(n+1)$th collision with the opposite components occurs.

(2) Collision with opposite components. For this case the map can be written as follows:

$$\begin{aligned}
\alpha^*_{n+1} &= \arcsin\left[\sin(\psi_n + \Phi) - \frac{x^*_{n+1}}{R}\cos\psi_n\right], \\
\alpha_{n+1} &= \alpha^*_{n+1}, \\
\varphi_{n+1} &= \psi_n - \alpha^*_{n+1}, \\
t_{n+1} &= t_n + \frac{R(\cos\varphi_n + \cos\varphi_{n+1} - 2\cos\Phi) + l}{V_n\cos\psi_n},
\end{aligned} \tag{7}$$

where

$$\begin{aligned}
\psi_n &= \alpha_n - \varphi_n, \\
x_n &= \frac{R}{\cos\psi_n}[\sin\alpha_n + \sin(\Phi - \psi_n)], \\
x^*_{n+1} &= x_n + l\tan\psi_n \pmod{a}.
\end{aligned}$$

These expressions follow from quite simple geometrical considerations which we omit.

2.3.2. Perturbed Boundary

Consider a billiard system with periodically perturbed focusing components. Suppose that the velocity value of the focusing component is the same in all points, and the velocity vector is directed by the normal to the component. Assume that the velocity value depends on time as follows:

$U(t) = U_0 p(\omega(t+t_0))$, where ω is a frequency oscillation and $p(\cdot)$ is a $2\pi/\omega$ periodic function. We study the case of $U_0/\omega \ll l$, i.e., the shift of the boundary is small enough so that it can be neglected. Therefore, the billiard map is written as follows:

$$\begin{aligned} V_n &= \sqrt{V_{n-1}^2 + 4V_{n-1}\cos\alpha_n^* U_n + 4U_n^2}\,, \\ \alpha_n &= \arcsin\left(\frac{V_{n-1}}{V_n}\sin\alpha_n^*\right), \end{aligned} \tag{8}$$

$$\left.\begin{aligned} \alpha_{n+1}^* &= \alpha_n, \\ \varphi_{n+1} &= \varphi_n + \pi - 2\alpha_n \pmod{2\pi}, \\ t_{n+1} &= t_n + \frac{2R\cos\alpha_n}{V_n}, \end{aligned}\right\} \quad \text{if} \quad |\varphi_{n+1}| \leqslant \Phi \tag{9}$$

$$\left.\begin{aligned} \psi_n &= \alpha_n - \varphi_n, \\ x_n &= \frac{R}{\cos\psi_n}[\sin\alpha_n + \sin(\Phi - \psi_n)], \\ x_{n+1}^* &= x_n + l\tan\psi_n \pmod{a}, \\ \alpha_{n+1}^* &= \arcsin\left[\sin(\psi_n + \Phi) - \frac{x_{n+1}^*}{R}\cos\psi_n\right], \\ \varphi_{n+1} &= \psi_n - \alpha_{n+1}^*, \\ t_{n+1} &= t_n + \frac{R(\cos\varphi_n + \cos\varphi_{n+1} - 2\cos\Phi) + l}{V_n\cos\psi_n}. \end{aligned}\right\} \quad \text{if} \quad |\varphi_n + \pi - 2\alpha_n| > \Phi \tag{10}$$

The given map describes a stadium-like billiard with the focusing components in the form of the circle arcs. This map is the exact one except for the approximation $U_0/\omega \ll l$. The first group (9) corresponds to the sequential multiple collisions with one of the focusing components, and the second group (10) corresponds to the passage to the opposite side of the boundary.

3. NUMERICAL ANALYSIS

In this Section we consider stadium-like billiards with the fixed and perturbed boundaries. In the first case, the particle dynamics is described by the approximate map (1) and exact map (6)–(7), respectively.

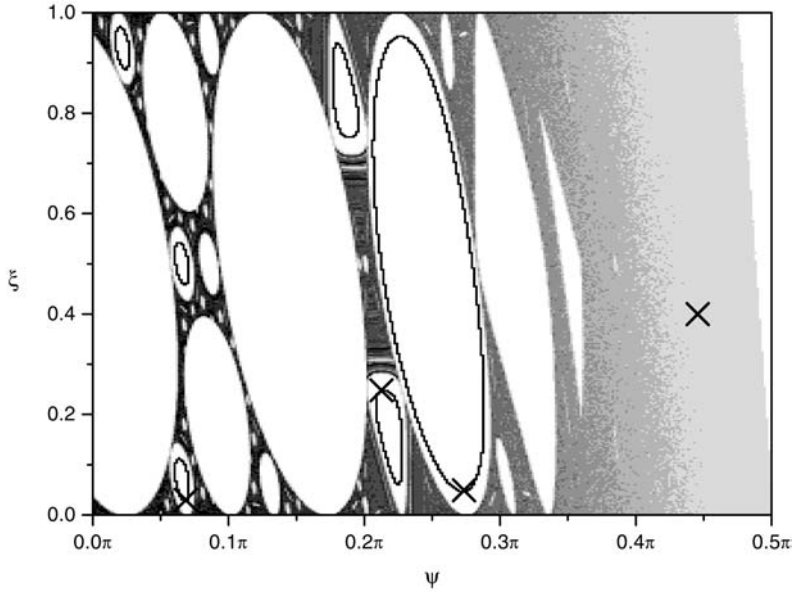

Fig. 5. Phase portrait of the stadium-like billiard with the focusing components in the form of the circle arcs (see map (6)–(7)). Parameters of the billiard are the same as in Fig. 2. One can see nonuniformity of the covering of the chaotic region.

3.1. Phase Diagrams of Billiards with the Fixed Boundaries

In Fig. 2, the phase diagram of the billiard with the fixed parabolic boundary is shown (see map (1)). Crosses in this figure are initial conditions. One can see that phase plane is divided into regular and chaotic regions. If the initial conditions belong to the regular region, then the trajectory lies on the corresponding invariant curves. However, for the initial conditions in chaotic region, the phase trajectory uniformly covers this region. The described portrait has been obtained on the basis of three regular trajectories (each contains 10^7 iterations) and only one chaotic trajectory ($5 \cdot 10^8$ iterations) of the map (1). Geometrical parameters of the billiard is the following: $a = 0.5,\ b = 0.01,\ l = 1$ (see Fig. 1).

In Fig. 5 similar results for the map (6)–(7), where the depth of the focusing components is taken into account, are shown. Remind that for this map the approximations $b \ll a$ and $b \ll l$ have not been used. To reasonable comparison, the geometric sizes of the billiard and the number of trajectories have been chosen the same as in the previous case (Fig. 2).

The difference between obtained diagrams can be easily explain by means of Fig. 6. Approximation of a small enough depth of the focusing

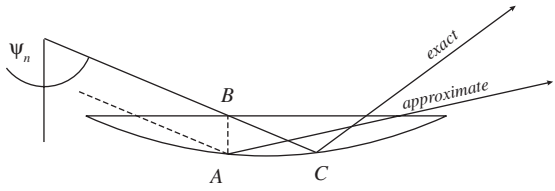

Fig. 6. The difference between the exact billiard map and the approximate map.

component for the map (1) means the following. Let B be an intersection point of the particle trajectory with a line connecting the ends of the focusing component. In approximation, we consider the particle collision in the point A which is a projection of B into the arc. But, in fact, the point C is the collision point. In this case, for a large enough ψ, collisions occur mainly with the right (in the figure) part of the arc, and from the collision to the collision the angle ψ decreases. Thus, the billiard particles as if "push out" to the region of small values of the angle ψ. This is in agreement with Fig. 5 where the region $\psi \lesssim \pi/2$ is empty.

The decrease in the density of trajectories for the large ψ corresponds to the known fact that in the chaotic billiards the distribution of the angle of incidence is in proportion to its cosine. In the stochastic layer (the right part of Fig. 5), approximation of numerical investigations gives a sufficiently good agreement with this result.

3.2. Perturbed Map

In this section we consider the problem of the velocity change near the resonance (4).

3.2.1. Phase Diagrams

Consider the map (8)–(10) of the perturbed stadium-like billiard. Construction of the phase diagrams has been performed for the same values of geometric parameters as in the previous Section 3.1. Therewith, the amplitude of oscillations is $U_0 = 0.01$. As noted above (see Section 2.2), for various particle velocities the corresponding phase portraits should be different form each other.

In Fig. 7 the resonance velocity as a function of the angle $\tilde{\psi}^m$ (see (4)) is shown. One can see that in the region form 0 to $\psi_{s\max}$ (where $\psi_{s\max}$ is a maximal angle for which the fixed points are still stable) the value of the resonance velocity is varied through a small range.

Phase portraits for the perturbed billiard are shown in Figs. 8 and 9. For detailed numerical analysis three particle ensembles with initial

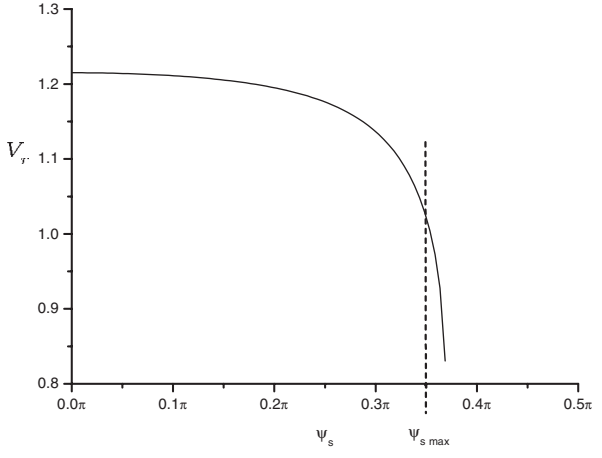

Fig. 7. The resonance velocity as a function of $\tilde{\psi}^m$ (see (4)).

value $V_0 = 1$, 1.2 and 1.5 have been considered. Therewith, initial conditions have been chosen in the chaotic region of the unperturbed billiard in a random way. When the difference between the particle velocity and V_0 exceeds 10%, the particle initialisation has been repeated. The phase space was divided into 300×300 cells. When the particle coordinates (ξ_n, ψ_n) are within some cell, its value is changed as $\Delta V_n = V_n - V_{n-1}$. Thus, the obtained portraits give an insight into the velocity dynamics of the billiard particle. In Figs. 8 and 9, the vertical shaded areas correspond to the velocity increasing, and the horizontal shaded areas fit its decreasing. The wait areas (without shading) are the intermediate ones; here the particle velocity is transient. The black tones correspond to the areas which are inaccessible for the phase trajectory.

As follows from the obtained diagrams, if V_0 is sufficiently far from V_r then around the stable fixed points there exist the areas surrounded by invariant curves. As before, these areas are inaccessible for particles from the chaotic regions. At the same time, in the neighbourhood which has became accessible for the particles as a result of perturbations, one can see areas of the increasing and the decreasing velocity. Depending on the relation to the resonance velocity value, they can change places.

If $V_0 \approx V_r$ (the resonance), then all neighbourhoods of the stable fixed points (except for the central one, $\psi_0 = 0$, $\xi_0 = 1/2$) become accessible for the trajectory. Moreover, for this resonance there are no the well-defined areas where the particles have an acceleration.

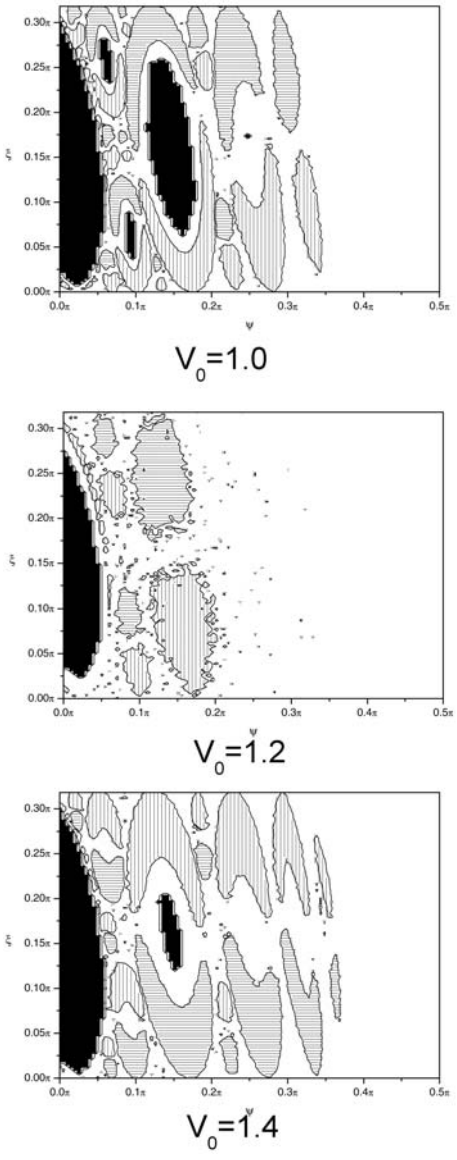

Fig. 8. Phase diagrams of the velocity change in the billiard with the perturbed boundary (see (8)–(10)) at $b = 0.01$, $a = 0.5$, $l = 1$, $U_0 = 0.01$ and $\omega = 1$. $V_0 = 1.0$, 1.2 (resonance), 1.5. Vertical shaded areas correspond to the velocity increasing, horizontal shaded zones symbolize its decreasing.

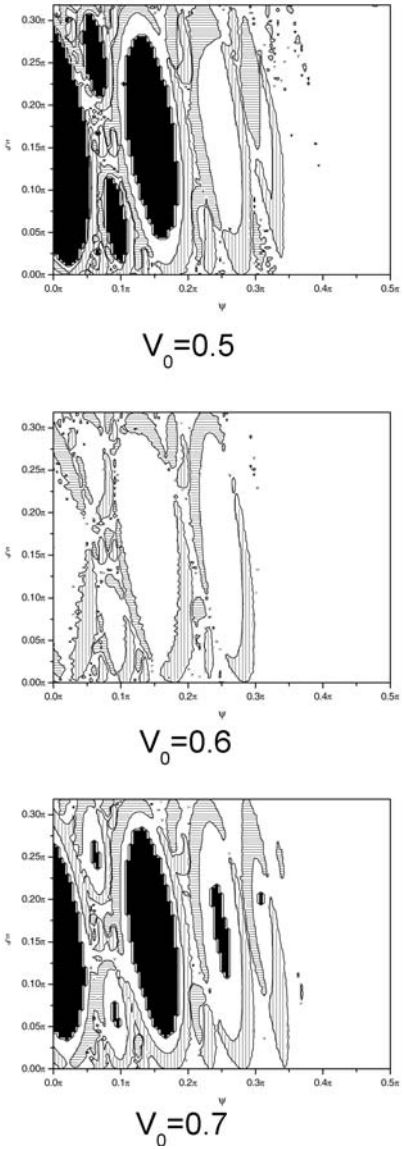

Fig. 9. The same as in Fig. 8 but $V_0 = 0.5$, 0.6 (resonance) and 0.7. Billiard parameters are the same as in Fig. 8.

Following (5), the resonance velocity in the neighbourhood of the central stable fixed points $V_r^0 \approx 0.6$. In Fig. 9 the phase diagrams for the initial velocities $V_0 = 0.5$, 0.6 and 0.7 are shown. One can see that at $V_0 = V_r^0$ all areas of the phase space are accessible. Moreover, if the initial velocity of the particles is a sufficiently near to V_r^0 (but not equal to it) then there exist areas corresponding to the increase and the decrease in the velocity. This is valid in neighborhoods of all fixed points. It is obvious that the reason is in the existence of the half-integer resonance between the rotation around the fixed point and the external perturbation.

3.2.2. The Particle Velocity as a Function of Iterations

Numerical investigations of the perturbed billiard described by the map (8)–(10) have been performed for two cases: when the billiard has strong chaotic properties and for a near-rectangle stadium. In the first case the billiard is a "classical" stadium. Then $\Psi = \pi/2$, and the billiard is a domain with the boundary that consists of two semicircles connected by the two parallel segments tangent to them. The latter case means that the focusing components are segments of the almost straight line, and the billiard system is a near-integrable one.

For the first case, the following billiard parameters were chosen as follows: $a = 0.5$, $b = 0.25$, $l = 1$, $u_0 = 0.01$, $\omega = 1$, and $V_0 = 0.1$. The particle velocity was calculated as the averaged value of the ensemble of 5000 trajectories with different initial conditions (solid curve 1 in Fig. 10). These initial conditions were different from each other by a random choice of the direction of the velocity vector V_0. As follows from the numerical analysis, the obtained dependence has approximately the square-root behaviour ($V(n) \sim \sqrt{n}$). The fitting function $y \sim an^c$ (the dot-and-dash curve 1 in Fig. 10) yields the following values: $a = 0.01015 \pm 0.00002$ and $c = 0.4446 \pm 0.0002$.

A near-integrable case means that parameter b (see Fig. 4) is a sufficiently small, and the curvature of the focusing components gives rise only weak nonlinearity in the system. In such a configuration the billiard phase space has regions with the regular and the chaotic dynamics. This case is much more interesting for investigations.

As follows from numerical analysis, there is a critical value V_c with the following properties. If the initial value $V_0 < V_c$ then the particle velocity decreases up to a certain quantity $V_{\text{fin}} < V_c$, and the particle distribution tends to the stationary one in the interval $(0, V_{\text{fin}})$. If, however, $V_0 > V_c$ then the billiard particles can reach high velocities. In this case the particle distribution is *not* stationary, and the mean velocity grows infinitely. Moreover, the average particle velocity is also not bounded.

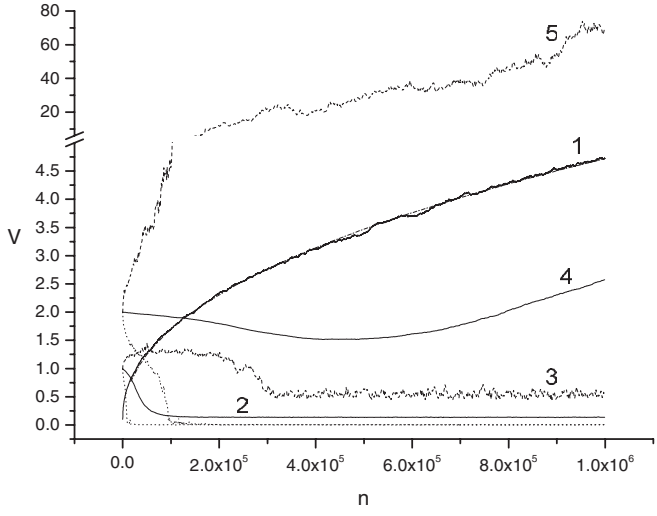

Fig. 10. Average velocity of the ensemble of 5000 particles in a stadium as a function of the number of collisions, $l = 1$, $a = 0.5$, $U_0 = 0.01$ and $\omega = 1$. Two (dot-dash and solid) curves 1 corresponds to the billiard with strong chaotic properties ($b = 0.25$). Curves 2–5 correspond to the near-integrable system ($b = 0.01$): $V_0 = 1$ (curve 2, 3) and $V_0 = 2$ (curve 4, 5). Curves 2 and 4 are the average velocities of the particle ensemble. Curves 3 and 5 correspond to maximal velocities reached by the particle ensemble to the nth iteration.

For detailed numerical investigations initial conditions were randomly chosen in the chaotic region of the corresponding unperturbed billiard. In Fig. 10 the average particle velocity as a function of the number of iterations is shown (curves 2–5). The billiard parameters remains the same as for the classical stadium (curve 1) except for $b = 0.01$. On the basis of 5000 realisations and for every initial velocity, *three curves* have been constructed: the average, minimal and maximal velocities which the particle ensemble has reached to the n-th iteration. So, we can see the interval of the velocity change. As follows from the figure, if $V_0 < V_c$ then the averaged particle velocity (solid curve 2) gradually decreases and tends to a constant. The maximal velocity of particles (dotted curve 3) also decreases up to V_{fin} and then fluctuate near this value. Eventually, the particle velocities lie in the interval $0 < V < V_{\text{fin}}$. In the case of $V > V_c$, the minimal velocity of particles decreases as before. This means that, in the ensemble, there is a number of particles which are in the region of low velocity values. In our numerical analysis the proportion of such particles was about 75%. At the same time, there are particles with high velocities (dashed curve 5, which corresponds to the maximal velocity of the ensemble). As a result, the averaged particle velocity (solid curve 4) increases.

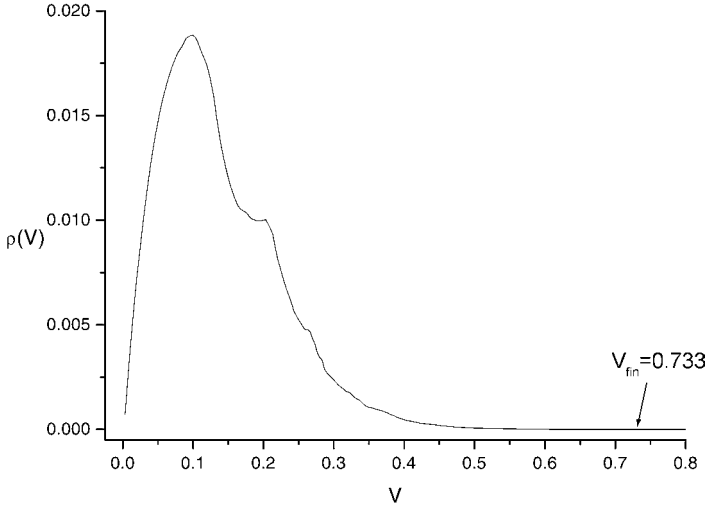

Fig. 11. Stationary distribution of the particle velocity calculated by the one-particle trajectory during 10^9 iterations. V_{fin} is a maximally reached velocity.

In Fig. 11 a stationary velocity distribution is shown. This distribution was calculated by the one-particle trajectory during 10^9 iterations. The initial velocity was chosen as follows: $V_0 \approx V_{\text{fin}}/2$. The value denoted by V_{fin} corresponds to the maximally reached velocity.

4. CONCLUDING REMARKS

Billiards are very convenient models of several physical systems. For example, particle trajectories in billiards of specific configuration can be used for modelling a lot of dynamical systems. Moreover, most approaches to the problems of mixing in many-body systems go back to billiard-like questions. A natural physical generalization of billiard systems is billiards whose boundaries are not fixed, but varies by a certain law. This is a quite new field which opens new prospects in the studies of problems that have been known for a long time.

In the present paper we have considered the problem of the billiard ball dynamics in a stadium with the periodically perturbed boundary. Numerical analysis showed that, for the case of the developed chaos (when the focusing components of the stadium are semicircles), the dependence of the particle velocity on the number of collisions has the root character. At the same time, for a near-rectangle stadium an interesting phenomena is observed. Depending on the initial values, the particle ensemble can be accelerated, or its velocity can decrease up to quite a low magnitude.

However, if the initial values do not belong to a chaotic layer then for quite high velocities the particle acceleration is not observed.

Analytical description of the considered phenomena requires more detailed analysis and will be published soon.[22]

ACKNOWLEDGMENTS

The authors would like to thank Professor Yakov Sinai for his interest in this work and valuable remarks.

REFERENCES

1. G. Birkhoff, *Dynamical Systems* (American Mathematical Society, N.Y., 1927).
2. J. Koiller, R. Markarian, S. Q. Kamphorst, and S. P. de Carvalho, Static and time-dependent perturbations of the classical elliptical billiard, *J. Statist. Phys.* **83**:127 (1996).
3. Ya. G. Sinai, Dynamical system with elastic reflection: Ergodic properties of dispersing billiards, *Russian Math. Surveys* **25**:137–188 (1970).
4. L. A. Bunimovich and Ya. G. Sinai, Statistical properties of Lorentz gas with periodic configuration of scatterers, *Comm. Math. Phys.* **78**:479–497 (1981).
5. R.Markarian. New ergodic billiards: Exact results, *Nonlinearity* **6**:819–841 (1993).
6. L. A. Bunimovich, On ergodic properties of some billiards, *Func. Anal. Appl.* **8**:73 (1974).
7. L. A. Bunimovich, On the ergodic properties of nowhere dispersing billiards, *Commun. Math. Phys.* **65**:295–312 (1979).
8. G. M. Zaslavsiky, Stochasticity in quantum mechanics, *Phys. Rep.* **80**:147–250 (1981).
9. S. M. Ulam, in *Proceedings of the 4th Berkeley Symp. on Math. Stat. and Probability* (University of California Press, 1961), Vol. 3, p. 315.
10. E. Fermi, On the origin of the cosmic radiation, *Phys. Rev.* **75**:1169 (1949).
11. A. J. Lichtenberg and M. A. Lieberman. *Regular and Stochastic Motion* (Springer-Verlag, Berlin, 1983).
12. J. Koiller, R. Markarian, S. Q. Kamphorst, and S. P. de Carvalho, Time-dependent billiards, *Nonlinearity* **8**:983 (1995).
13. A. Ibort, M. de Leon, E. A. Lacomba and others, Geometric formulation of mechanical systems subjected to time-dependent one-sided constraints, *J. Phys. A* **31**:2655 (1998).
14. M. Levi, Quasiperiodic motions in superquadratic time-periodic potentials, *Commun. Math. Phys.* **143**:43–83 (1991).
15. S. Q. Kamphorst and S. P. de Carvalho, Bounded gain of energy on the breathing circle billiard, *Nonlinearity* **12**:1363, (1999).
16. A. Loskutov, A. B. Ryabov, and L. G. Akinshin, Mechanism of Fermi acceleration in dispersing billiards with time-dependent boundaries, *J. Experiment. Theoret. Phys.* **86**:966–973 (1999).
17. A. Loskutov, A. B. Ryabov, and L. G. Akinshin, Properties of some chaotic billiards with time-dependent boundaries, *J. Phys. A* **44**:7973–7986 (2000).
18. M. A. Porter and R. L. Liboff, Vibrating quantum billiards on Riemannian manifolds, *Internat. J. Bifur. Chaos* **11**:2305–2315 (2001).

19. M. A. Porter and R. L. Liboff, Quantum chaos for the vibrating rectangular billiard, *Internat. J. Bifur. Chaos* **11**:2317–2337 (2001).
20. M. A. Porter and R. L. Liboff, Quantum chaos for the radially vibrating spherical billiard, *Chaos* **10**:366–370 (2000).
21. L. A. Bunimovich, Conditions of stochasticity of two-demensional billiards, *Chaos* **1**:187–93 (1991).
22. A. Loskutov and A. B. Ryabov, To be published.